euronoise

Recent progress of acoustic microscopy for medicine and biology

Yoshifumi Saijo[a], Kazuto Kobayashi[b], Takahiro Iwamoto[a], Nagaya Okada[b], Akira Tanaka[c] and Naohiro Hozumi[d]

[a]Tohoku University, 4-1 Seiryomachi, Aoba-ku, 980-8575 Sendai, Japan
[b]Honda Electronics Co. Ltd., 20 Oyamazuka, Oiwa-cho, 441-3193 Toyohashi, Japan
[c]Fukushima University, 1 Kanayagawa, 960-1296 Fukushima, Japan
[d]Aichi Institute of Technology, 1247 Yachigusa, Yakusa-cho, 470-0392 Toyota, Japan
saijo@idac.tohoku.ac.jp

Conventional acoustic microscopy with only C-mode imaging has widened its data acquisition mode to B-mode, C-mode, surface acoustic impedance mode and three-dimensional (3D) mode. The base of our acoustic microscope system was consisted of (1) PVDF transducer with the central frequency of 100 MHz, (2) ultrasonic pulser made of high speed semiconductor switching, (3) mechanical scanner using two linear servo motors, (4) high speed PCI card digitizer with the sampling frequency of 2 GHz, and (5) personal computer controlling the whole system.

1 Introduction

Conventional scanning acoustic microscopy for medicine and biology has been developed for more than twenty years at Tohoku University [1-9]. Recently, dramatic shortening of the calculation time has been provided by the progress of the computer technology and it has made biomedical researchers to possibly assess the non-linear acoustic phenomena in soft materials which had been assumed as acting linearly. Besides, the spread of Windows-based personal computer and peripheral devices enabled easier and cheaper configuration of the whole acoustic microscope system such as pulse generation, analogue/digital conversion, mechanical scanning and image processing.

In the present study, conventional acoustic microscopy with only C-mode imaging has widened its data acquisition mode to B-mode, C-mode, surface acoustic impedance mode and three-dimensional (3D) mode. Regenerated skin model and fingerprint were visualized by the ultrasound imaging system.

2 Methods

2.1 Instrumentation

The following system was commonly used for each imaging mode. An electric impulse was generated by a high speed switching semiconductor. The start of the pulse was within 400 ps, the pulse width was 2 ns, and the pulse voltage was 40 V. The frequency of the impulse covered up to 500 MHz. The electric pulse was used to excite a PVDF transducer with the central frequency of 100 MHz. The ultrasound spectrum of the reflected ultrasound was broad enough to cover 50-160 MHz (-6dB). The reflections from the tissue was received by the transducer and were introduced into a Windows-based PC (Pentium D, 3.0 GHz, 2GB RAM, 250GB HDD) via a high-speed A/D converter (Acqiris DP210, Geneva, Switzerland). The frequency range was 500 MHz, and the sampling rate was 2 GS/s. Eight pulse echo sequences were averaged for each scan point in order to increase the signal-to-noise-ratio. The transducer was mounted on an X-Y stage with a microcomputer board that was driven by the PC through RS232C. The Both X-scan and Y-scan were driven by linear servo motors. Fig. 1 shows the schematic illustration of the system.

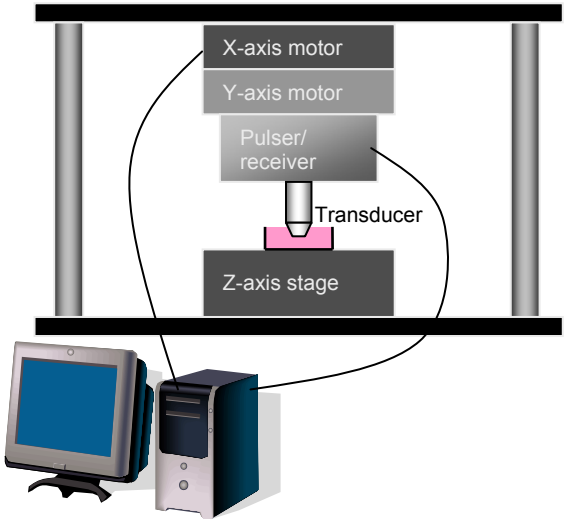

Fig.1 Schematic illustration of the ultrasound imaging system

2.2 Instrumentation

Surface and 3D-mode imaging was obtained with a PVDF transducer with the diameter of 2.4 mm and the focal length of 3.2 mm. C-mode imaging was obtained with a different PVDF transducer with the diameter of 1.8 mm and the focal length of 1.5 mm. Figure 2 shows the characteristics of the sound field of two kinds of transducers.

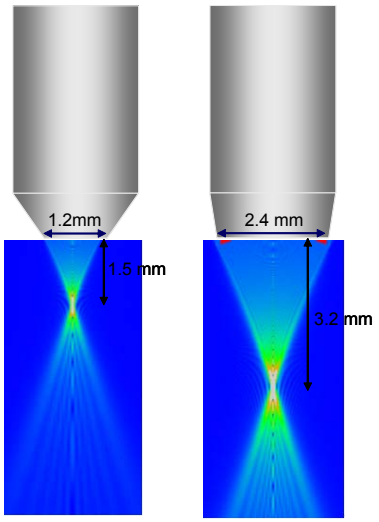

Fig.2 Comparison of the two kinds of ultrasonic transducers

2.3 Regenerated skin model

In the present study, cultured 3D skin model Vitrolife-Skin® (Gunze, Kyoto, Japan) was used for conventional acoustic microscopy. Vitrolife-Skin® was a 3D human skin model used as an alternative for animal skin during irritation test. Keratinocytes were cultured to cover cultured epidermis to form two-layered structure [10]. Fig.3 shows the schematic illustration of the 3D skin model.

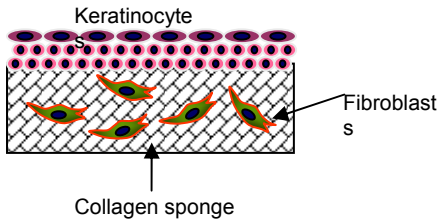

Fig.3 Schematic illustration of Vitrolife-Skin®

For B-mode, surface acoustic impedance mode and 3D mode, human finger was scanned by the system. Water was used as the coupling medium between the transducer and the finger.

2.4 Signal processing for C-mode

Denoting the standardized phase of the reflection wave at the tissue surface as ϕ_{front}, the standardized phase at the interference between the tissue and the substrate as ϕ_{rear},

$$2\pi f \times \frac{2d}{c_o} = \phi_{front} \qquad (1)$$

$$2\pi f \times 2d\left(\frac{1}{c_o} - \frac{1}{c}\right) = \phi_{rear} \qquad (2)$$

where d is the tissue thickness, c_o is the sound speed in coupling medium and c is the sound speed in the tissue. Thickness is obtained as

$$d = \frac{c_o}{4\pi f}\phi_{front} \qquad (3)$$

Finally, sound speed is calculated as

$$c = \left(\frac{1}{c_o} - \frac{\phi_{rear}}{4\pi fd}\right)^{-1} \qquad (4)$$

After determination of the thickness, attenuation of ultrasound was then calculated by dividing amplitude by the thickness and frequency.

2.5 Signal processing for surface acoustic impedance mode

The target signal is compared with the reference signal and interpreted into acoustic impedance as

$$Z_{target} = \frac{1-\frac{S_{target}}{S_0}}{1+\frac{S_{target}}{S_0}} Z_{sub} = \frac{1-\frac{S_{target}}{S_{ref}}\cdot\frac{Z_{sub}-Z_{ref}}{Z_{sub}+Z_{ref}}}{1+\frac{S_{target}}{S_{ref}}\cdot\frac{Z_{sub}-Z_{ref}}{Z_{sub}+Z_{ref}}} Z_{sub} \cdots (5)$$

where S_0 is the transmitted signal, S_{target} and S_{ref} are reflections from the target and reference, Z_{target}, Z_{ref} and Z_{sub} are the acoustic impedances of the target, reference and substrate, respectively [11].

Fig.4 shows the schematic illustration of surface acoustic impedance mode.

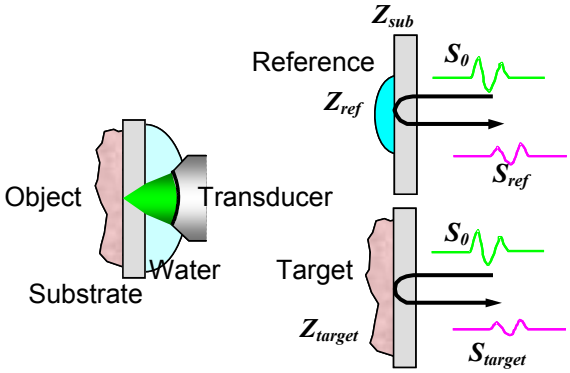

Fig.4 Schematic illustration of surface acoustic impedance mode

In case of using water as the reference, its acoustic impedance was assumed to be 1.5 x 10^6 Ns/m^3. On the other hand, in case of using silicon rubber, the acoustic impedance of itself was calibrated, by using water as the standard reference material. In this report, 0.965 x 10^6 Ns/m^3 was used. The acoustic impedance of the substrate was calculated to be 3.22 x 10^6 Ns/m^3, considering its sound speed and density.

2.6 Signal processing for B-mode and 3D-mode

RF signal of each scanning line was converted to B-mode image by a conventional image processing algorithm. The scan area was 2.4 mm x 3.0 mm with 300 x 4000 pixels. Y scan width was available 8 / 16 / 24 / 64 microns step to obtain 3D data set. 3D image was obtained by 3D reconstruction of the consecutive images.

3 Results

3.1 C-mode imaging of Vitrolife-Skin®

Fig.5 shows the (a) optical microscopic and (b) C-mode (sound speed) image of Vitrolife-Skin®. The sound speed of the epidermis was approximately 1580 m/sand the sound speed of dermis was ranged 1530 to 1560 m/s corresponding to the density of fibroblasts in the dermis.

(a)

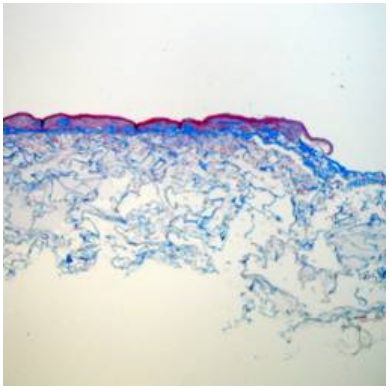

(b)

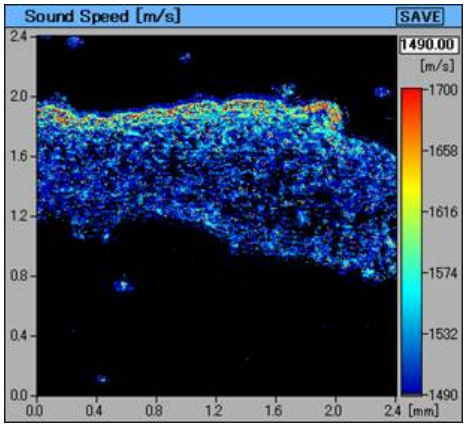

Fig.5 (a) optical microscopic and (b) C-mode (sound speed) image of Vitrolife-Skin®

3.2 Surface acoustic impedance mode

Fig.6 shows the surface acoustic impedance mode og human fingerprint. Besides the friction ridges of the surface of the finger, pores of eccrine glands (white arrows) are clearly observed.

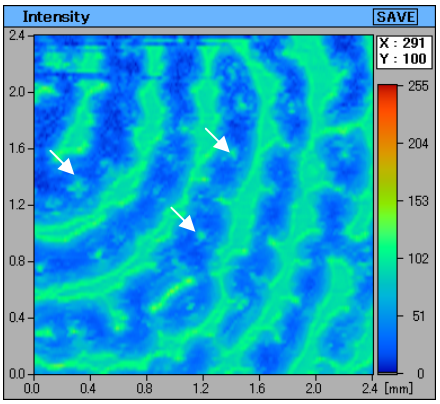

Fig.6 Surface acoustic impedance mode of human fingerprint

3.3 B-mode imaging of human fingerprint

Fig.7 shows (a) B-mode and (b) corresponding histology of the human fingerprint. The friction ridges of the finger are clearly shown in the B-mode image.

(a)

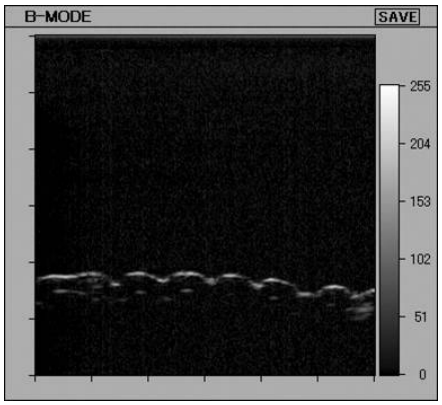

(b)

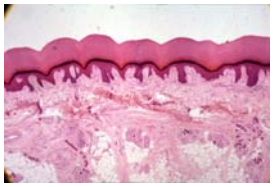

Fig.7 (a) B-mode and (b) corresponding histology of the human finger print

3.4 3D-mode imaging of human fingerprint

Fig.8 shows 3D acoustic microscope image of the finger print of (a) surface and (b) rear surface. Besides the friction ridges shown in surface image, dermal papillae with eccrine glands are clearly shown in rear surface image.

(a)

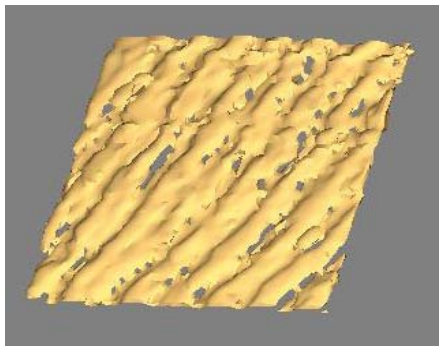

(b)

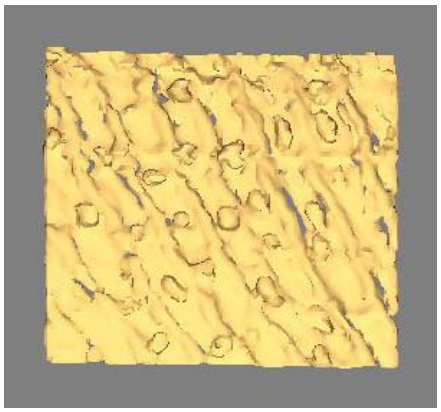

Fig.8 3D imaging of the fingerprint of (a) surface and (b) rear surface

4 Discussion

Compared with conventional acoustic microscopes, this system is unique because the system is capable of imaging the tissue in three different modes; (1) conventional C-mode acoustic microscope imaging of thinly sliced tissue, (2) ultrasound impedance imaging of the surface of tissue, (3) B-mode imaging of the tomography of the tissue and (4) 3D ultrasound imaging of the whole tissue. Especially, surface impedance imaging and 3D imaging have realized the use of acoustic microscopy *in vivo* and in clinical settings. As the spatial resolution of the system is 15 micron, it is enough to visualize epidermis with 50-100 micron thickness and friction ridges of the fingerprint were clearly visualized by the system.

3D imaging would provide direct information on the cancer invasion of in the dermal layer to hypodermal layer. As the original RF signal was accessible in the system, automatic tissue classification methods established in intravascular ultrasound [12-13] would be applicable to the diagnosis of the skin.

5 Conclusion

An acoustic microscope system with C-mode, surface acoustic impedance mode, B-mode, and three-dimensional (3D) imaging was developed. For skin imaging, conventional C-mode imaging of thinly sliced skin sample presented quantitative values of sound speed. Surface acoustic impedance imaging of the fingerprint can be obtained by just putting a finger on a thin plastic plate of the transducer. 3D imaging of the fingerprint was reconstructed by consecutive B-mode imaging.

Acknowledgments

This work was supported in part by Grants from New Energy and Industrial Technology Development Organization (06001905-0), Sendai Advanced Preventive Health Care Services Cluster from the Ministry of Education, Culture, Sports, Science and Technology, and Grants-in-Aid for Scientific Research (Scientific Research (B) 19300179) from the Japan Society for the Promotion of Science.

References

[1] M. Tanaka, H. Okawai, N. Chubachi, J. Kushibiki, T. Sannomiya, "Propagation properties of ultrasound in acoustic microscopy through a double-layered specimen consisting of thin biological tissue and its holder," *Jpn J Appl Phy 23*, 197-199 (1984)

[2] Y. Saijo, M. Tanaka, H. Okawai, F. Dunn, "The ultrasonic properties of gastric cancer tissues obtained with a scanning acoustic microscope system," *Ultrasound Med Biol 17*, 709-714 (1991)

[3] H. Sasaki, M. Tanaka, Y. Saijo, H. Okawai, Y. Terasawa, S. Nitta, K. Suzuki, "Ultrasonic tissue characterization of renal cell carcinoma tissue," *Nephron 74*, 125-130 (1996)

[4] Y. Saijo, M. Tanaka, H. Okawai, H. Sasaki, S. Nitta, F. Dunn, "Ultrasonic tissue characterization of infarcted myocardium by scanning acoustic microscopy," *Ultrasound Med Biol 23*, 77-85 (1997)

[5] Y. Saijo, H. Sasaki, H. Okawai, S. Nitta, M. Tanaka, "Acoustic properties of atherosclerosis of human aorta obtained with high-frequency ultrasound," *Ultrasound Med Biol 24*, 1061-1064 (1998)

[6] Y. Saijo, H. Sasaki, M. Sato, S. Nitta, M. Tanaka, "Visualization of human umbilical vein endothelial cells by acoustic microscopy," *Ultrasonics 38*, 396-399

[7] Y. Saijo, T. Ohashi, H. Sasaki, M. Sato, C.S. Jorgensen, S. Nitta, "Application of scanning acoustic microscopy for assessing stress distribution in atherosclerotic plaque," *Ann Biomed Eng 29*, 1048-53

[8] Y. Saijo, T. Miyakawa, H. Sasaki, M. Tanaka, S. Nitta, "Acoustic properties of aortic aneurysm obtained with scanning acoustic microscopy," *Ultrasonics 42*, 695-698 (2004)

[9] H. Sano, Y. Saijo, S. Kokubun, "Material properties of the supraspinatus tendon at its insertion – A measurement with the scanning acoustic microscopy," *J Musculoskeletal Res 8*, 29-34 (2004)

[10] T. Uchino, H. Tokunaga, H. Onodera, M. Ando, "Effect of squalene monohydroperoxide on cytotoxicity and cytokine release in a three-dimensional human skin model and human epidermal keratinocytes," *Biol Pharm Bull 25*, 605-10 (2002)

[11] N. Hozumi, A. Kimura, S. Terauchi, M. Nagao, S. Yoshida, K. Kobayashi & Y. Saijo, "Acoustic impedance micro-imaging for biological tissue using a focused acoustic pulse with a frequency Range up to 100 MHz," *Proc 2005 IEEE Int Ultrason Symp* 170-173 (2005)

[12] Y. Saijo, A. Tanaka, N. Owada, Y. Akino, S. Nitta, "Tissue velocity imaging of coronary artery by rotating-type intravascular ultrasound," *Ultrasonics 42*, 753-757 (2004)

[13] Y. Saijo, A. Tanaka, T. Iwamoto, E. D. Santos Filho, M. Yoshizawa, A. Hirosaka, M. Kijima, Y. Akino, Y. Hanadate, T. Yambe, "Intravascular two-dimensional tissue strain imaging," *Ultrasonics 44*, e147-151 (2006)